

Magnetic models on Apollonian networks

Roberto F. S. Andrade

*Instituto de Física,
Universidade Federal da Bahia,*

Hans J. Herrmann*

*Departamento de Física,
Universidade Federal do Ceará,
60450 Fortaleza, CE, Brazil*

(Dated: March 23, 2018)

Abstract

Thermodynamic and magnetic properties of Ising models defined on the triangular Apollonian network are investigated. This and other similar networks are inspired by the problem of covering an Euclidian domain with circles of maximal radii. Maps for the thermodynamic functions in two subsequent generations of the construction of the network are obtained by formulating the problem in terms of transfer matrices. Numerical iteration of this set of maps leads to exact values for the thermodynamic properties of the model. Different choices for the coupling constants between only nearest neighbors along the lattice are taken into account. For both ferromagnetic and anti-ferromagnetic constants, long range magnetic ordering is obtained. With exception of a size dependent effective critical behavior of the correlation length, no evidence of asymptotic criticality was detected.

PACS numbers: 05.50.+q, 89.75.Hc, 02.50.Cw, 64.60.Ak.

*Also at Institute for Computerphysics,

University of Stuttgart, Germany

email: hans@ica1.uni-stuttgart.de

I. INTRODUCTION

The investigation of magnetic models on scale invariant networks has attracted the attention of scientists since the 80's [1, 2]. Besides the fact that, on such graphs, renormalization procedures can lead to exact results[3], they have been explored as models for systems that are not translational invariant, neither in the positions of the spins nor in the coupling constants mediating the interactions between them. In this respect, the analysis of disordered and aperiodic models on scale invariant graphs, which include hierarchical lattices[4, 5, 6], Cayley trees [7] or Sierpinski gaskets and carpets[8, 9], have provided valuable insight into the behavior of critical phenomena of non homogeneous systems on Euclidean lattices.

A further family of scale invariant graphs are Apollonian networks, the simplest of which is illustrated in Fig. 1. This lattice can be defined based of the ancient problem of filling space with spheres, first tackled by the Greek mathematician Apollonius of Perga [10]. In its two dimensional version, corresponding to the problem of the plane filled by circles, the nodes of this network are defined by the positions of the centers of the circles, while edges are drawn between any pair of nodes corresponding to pairs of touching circles[11]. The resulting network, corresponds to the contact force network of the packing[12]. Apollonian networks can also be used to describe generically other scale-free situations like space-filling porous media [13] or the connections between densely located cities on which one is interested in fluid flow, car traffic or electric supply. Therefore it is useful to study not only the geometric properties of Apollonian networks but also transport and ordering on them.

In a previous paper [14], we analyzed several of its properties. In particular, we have shown that it has small-world properties, a scale-free degree distribution, a very high clustering coefficient and a very short diameter, all this having been confirmed independently by Doye [15]. Moreover, the Apollonian network can be embedded in the Euclidian plane, what is not the case for other scale invariant lattices, e.g. hierarchical lattices or Cayley trees. One can of course define other similar lattices based on modified packing rules [16]. Although the numerical values for exponents depend on the topology of each realization, basic properties characterizing complex networks remain the same.

In our first work, we have also devoted our attention to several physical models on the Apollonian network (electrical resistance, percolation, magnetic ordering), pointing out the most striking features. In this work, we review our investigations on the properties of several

Ising models on the Apollonian network, and present a thorough discussion, regarding on one hand some of the details of the Transfer Matrix (TM) methods and, on the other hand, the most important thermodynamic and magnetic properties. Several choices for rules defining the values of the coupling constants are considered, including both ferro (F)- and anti-ferromagnetic (AF) interactions. As will be shown, we found long range magnetic ordering for almost all choices of couplings without any noticeable evidence of a phase transition to a paramagnetic phase at a finite temperature. For particular choices of F and AF bonds, the geometry of the network induces the presence of competition and frustration within closed loops of odd number of sites, giving rise to residual entropy and changes in the correlation length. The behavior of this quantity deserves a detailed discussion, as it points to a transition from long to short range correlation only for finite size systems, in a similar way as discussed for magnetic models on scale-free lattices[17]

The rest of this paper is organized as follows: in Section II we discuss our models. In Section III we obtain the maps for the free energy and its derivatives, as well as for the correlation length. Results are discussed in Section IV, while concluding remarks are presented in Section V.

II. ISING MODELS

The Apollonian network is constructed recursively. In each generation, it incorporates a new set of sites, which correspond to the centers of the new circles added to the packing filling the holes left in the previous generation. In the present work we consider the lattice which starts with three touching circles drawn on the vertices of an equilateral triangle, and the packing problem is restricted to filling the space bounded by these three initial circles, as shown in Figure 1a. If n denotes the current generation of the network, the number of sites $N(n)$ is asymptotically three times that of the previous generation, i.e. $N(n+1) = 3N(n) - 5$, or $N(n) = (3^{n-1} + 5)/2$. The number of edges linking nodes increases with n according to $B(n+1) = B(n) + 3(N(n+1) - N(n))$. As a consequence, $B(n) = (3 + 3^n)/2$, $B(n)/N(n) \rightarrow 3$ in the limit of large n , so that on average, each site is linked to six other sites, which is the coordination number of the triangular lattice.

Once the Apollonian network has been defined, it is possible to define many different models on it. In this work we focus on a set of interacting Ising spins $s_i = \pm 1$ placed on

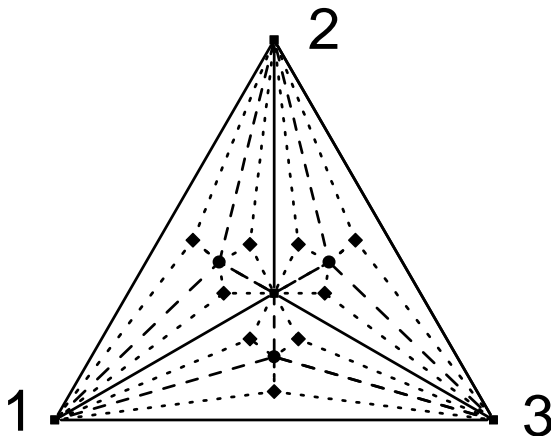


FIG. 1: Third generation of construction of the Apollonian network. Sites represented by squares, circles and diamonds are introduced in the first, second and third generation. Links represented by dotted, dashed and solid lines correspond to $n = 1, 2$ and 3 in eq(8).

each site of the network. Interactions are restricted to pairs of spins placed on nodes linked by edges, as described in the Introduction. So, some spins placed far apart may interact, while pairs of spins placed relatively close to each might not. This can be of interest to model special disordered systems, having interactions of all ranges.

For the packing problem, it is important to calculate the radius of each circle $c(i, n)$, which depends both on the generation n as well as on the local environment, i.e., the generations of the three circles that it touches $n_p(i, k), k = 1, 2, 3$. It is possible to include this dependence into the magnetic model, by defining coupling constants (or local fields) depending on the distance between nodes, i.e., $J(n, i, n_p(i, j))$. We restrict ourselves, however, to a simpler situation, where the coupling constants J only depend on the generation n at which the edge was introduced into the network. In Figure 1b we illustrate the first three steps of the construction of the model.

To have a physically interesting model, it may be reasonable to choose values for J that increase with n . Indeed, when n increases, the average length of the edges introduced in that generation decreases and, as the spins get closer, we might expect that the interactions among them become stronger. However, to avoid the divergence of the energy within the lattice, it is necessary to renormalize the value of all J 's as n increases. To accomplish this, we define $J_{n,m}, m = 1, \dots, n$ as the value of the constant introduced in the m -th generation,

when the lattice has been built up to its n -th generation, and require that $J_{n,m}$ decreases with $n - m$. A sufficiently general choice would be

$$J_{n,m} = \frac{(\pm 1)^m J_0}{(n - m + 1)^\alpha}, \quad (1)$$

where J_0 may have ferro- (> 0) or antiferromagnetic (< 0) character, the exponent α controls how the interactions decay with the difference $n - m$, and yields a possibility of choosing the interactions according to the generation at which they were introduced.

One of the extreme situations, $\alpha = 0$, corresponds to equal interactions along all edges in the network. On the other hand, in the $\alpha \rightarrow \infty$ limit, the model contains only finite interactions for the subset of edges that were introduced in that last generation n , as illustrated in Figure 1b. The number of these surviving bonds is given by $B(n) - B(n - 1) = 3^{n-1}$, so that the average coordination number is reduced to four. Moreover, the lattice is then composed by four-sided polygons, so that competition and frustration due to the presence of antiferromagnetic bonds can never occur in this α limit.

To close this section we write down the formal Hamiltonian of this model

$$H_n = - \sum_{(i,j)} \overline{J_{i,j}} s_i s_j - h \sum_i s_i, \quad (2)$$

where all pairs of nearest neighbors denoted by (i, j) are defined according to the construction rules of the network, and the constants $\overline{J_{i,j}}$ must be chosen from the set defined in eq.(1) according to the value of m in which the edge was introduced. We also include a constant magnetic field h , which allows for the evaluation of magnetic properties. The notation in eq.(2) does not include the selection of the bonds that are taken into account. The evaluation of a partition function can in fact be set up in much proper terms through the transfer matrix formalism.

III. TRANSFER MATRIX AND RECURRENCE RELATIONS

The numerical evaluation of the partition function for magnetic models on scale invariant graphs with a finite number of end nodes has been performed with the help of TM derived maps for a large number of lattices and models. The problem we are interested in this work is also suitable to be analyzed within this framework. For the sake of simplicity, let us first consider the homogeneous case $\alpha = 0$, and set $h = 0$. If we consider the first generation

$n = 1$, we observe that a 2×2 TM M_1 , which takes into account all interactions between the sites i and k of Figure 1 can be written as:

$$M_1 = \begin{pmatrix} a_1 & b_1 \\ b_1 & a_1 \end{pmatrix} = \begin{pmatrix} a(a^2 + b^2) & 2ab^2 \\ 2ab^2 & a(a^2 + b^2) \end{pmatrix}, \quad (3)$$

where $a = b^{-1} = \exp(\beta J_0)$. M_1 can be used to describe one single cell or a linear chain of triangles that are connected by their bases. It is also possible to define a 2×4 TM L_1 , that describes the interactions among sites i, j and k , where the column labels κ are composed from the pair (j, k) according to the lexicographic order, i.e., $\kappa = 2(j - 1) + k$ according to

$$L_1 = \begin{pmatrix} c_1 & d_1 & d_1 & d_1 \\ d_1 & d_1 & d_1 & c_1 \end{pmatrix} = \begin{pmatrix} a^3 & ab^2 & ab^2 & ab^2 \\ ab^2 & ab^2 & ab^2 & a^3 \end{pmatrix}. \quad (4)$$

Of course we note that $a_1 = c_1 + d_1$ and $b_1 = 2d_1$.

Within the proposed framework, all interactions between the sites i and k , for any higher order generations $n = 2, 3, 4, \dots$, should be written in terms of a single 2×2 TM's M_n , with the same distribution of matrix elements as M_1 . Moreover, the matrix elements of M_n should be written in terms of those of the matrices of the lower generation $n - 1$ only. This turns out to be feasible since the Apollonian lattice, in a generation $n + 1$, can be decomposed into three sublattices, each one of them being a deformed lattice of generation n . Since the coupling constants do not depend on the actual distance between the sites, each of the three sublattices entails the same coupling constants and magnetic structure as the n -lattice. Thus, a matrix M_{n+1} can indeed be written in terms of three matrices M_n . To achieve this we remark that, in any generation, the three sublattices share their three outmost sites, which we label as i, j, k and ℓ . This last one occupies the geometrical center of the $n + 1$ -lattice. Then, M_{n+1} can be defined using

$$(M_{n+1})_{i,k} = \sum_{j,\ell} (L_n)_{i,j\ell} (L_n)_{i,\ell k} (L_n^t)_{k,j\ell}. \quad (5)$$

and

$$(L_{n+1})_{i,jk} = \sum_{\ell} (L_n)_{i,j\ell} (L_n)_{i,\ell k} (L_n^t)_{k,j\ell}. \quad (6)$$

As one can easily observe by direct evaluation of eq.(5) and eq.(6), all matrices M_n and L_n , share the same matrix element distribution as M_1 and L_1 . So, it is possible to immediately

write down recurrence relations for the elements of L_{n+1} in terms of those of L_n as

$$\begin{aligned} c_{n+1} &= c_n^3 + d_n^3 \\ d_{n+1} &= c_n d_n^2 + d_n^3, \end{aligned} \tag{7}$$

from which the elements $a_{n+1} = c_{n+1} + d_{n+1}$ and $b_{n+1} = 2d_{n+1}$ can be obtained.

However, a direct evaluation of the matrix elements defined by the equations (5)-(7) shows that they do not exactly describe the interactions between the sites i and k . For instance, in the generation $n = 2$, the number of magnetic bonds is equal to the number of edges $B(n = 2) = 6$. On the other hand, we see that the Boltzmann weights in M_2 are expressed by combinations of $\exp(\beta r J_0) \exp(-\beta s J_0)$, with $r + s = 9$ instead of $r + s = 6$. This is due to the fact that each one of the interactions between the site ℓ and its neighbors i, j and k appears twice in eq.(5). To describe the thermodynamics of the system with the help of equations (5)-(7), it is necessary to carry out a small correction, namely to redefine a and b as $a = b^{-1} = \exp(\beta J_0/2)$. With this modification, the Boltzmann weights in each element are expressed by exponentials of $\beta(r - s)J_0$, where $r + s = B(n) - 3/2$. So, for each spin configuration, the ratio between the correct energy and that one provided by equations (5) and (6) is roughly proportional to $(B(n) - 3/2)/B(n)$, which $\rightarrow 1$ in the limit $n \rightarrow \infty$.

These definitions are sufficient for only the uniform interaction model $\alpha = 0$. Further modifications in eqs.(5)-(7) are required to obtain the correct maps for general α . To cast this into a single recurrence relation, we first note that it is not necessary to use two labels n and m to insert the correct coupling constants into M_n . As these matrices are recursively defined, the largest and most abundant $J_{n,n}$ corresponds to the constant introduced into M_1 , which is reproduced in ever growing number by the successive use of equations like (5)-(6). On the other hand, the smallest and least frequent $J_{n,1}$ represents the constant that is inserted into the sequence of TM's exactly at the n -th generation. So we consider

$$J_{n,m} \rightarrow \mathbf{J}_n = \frac{(\pm 1)^n J_0}{(n - 1)^\alpha}. \tag{8}$$

Note that the changes carried into the denominator of eq.(8) set $\mathbf{J}_1 = 0$, and $\mathbf{J}_{n+1} \rightarrow \mathbf{J}_n$. This strategy is necessary to avoid taking into account more than once the effect of bonds introduced when $n = 1$, and it is somehow equivalent to the redefinition of a and b discussed above.

Then we modify equations (5) and (6) according to

$$(M_{n+1})_{i,k} = \sum_{j,\ell} (L_n)_{i,j\ell} (L_n)_{i,\ell k} (L_n^t)_{k,j\ell} (C_n)_{i,\ell} (C_n)_{\ell,j} (C_n)_{\ell,k} \quad (9)$$

and

$$(L_{n+1})_{i,k} = \sum_{\ell} (L_n)_{i,j\ell} (L_n)_{i,\ell k} (L_n^t)_{k,j\ell} (C_n)_{i,\ell} (C_n)_{\ell,j} (C_n)_{\ell,k}, \quad (10)$$

where the 2×2 TMs C_n are defined by

$$C_n = \begin{pmatrix} p_n & q_n \\ q_n & p_n \end{pmatrix} = \begin{pmatrix} \exp(\beta \mathbf{J}_n) & \exp(-\beta \mathbf{J}_n) \\ \exp(-\beta \mathbf{J}_n) & \exp(\beta \mathbf{J}_n) \end{pmatrix}. \quad (11)$$

With these definitions, it is possible to observe that the number of non-zero coupling constants in the lattice is $B(n) - 3$ so that, in the $n \rightarrow \infty$ limit, equations (8)-(11) accurately describe the thermodynamic properties of the model. The recurrence maps for the matrix elements derived from (9)-(10) read

$$\begin{aligned} c_{n+1} &= c_n^3 p_n^3 + d_n^3 q_n^3 \\ d_{n+1} &= c_n d_n^2 p_n^2 q_n + d_n^3 p_n q_n^2 \end{aligned} \quad (12)$$

From equations (7) or (11) it is possible to derive recurrence maps for the free energy $f_n = -T \ln(c_n + d_n)/N(n)$ and correlation length $\xi_n = 1/\ln((c_n + d_n)/(c_n - d_n))$ at two subsequent generations, $f_{n+1} = f_{n+1}(f_n, \xi_n; T)$ and $\xi_{n+1} = \xi_{n+1}(f_n, \xi_n; T)$ can easily be derived [18, 19]. This set of maps can be increased by working out explicit recurrence relations for the derivatives of $f_n(T)$ with respect to both the temperature and the magnetic field, obtaining the entropy $s(T)$, the specific heat $c(T)$, the spontaneous magnetization $m(T) = m(T, h = 0)$, and the magnetic susceptibility $\chi(T, h = 0)$. For this last purpose, we have to consider $h \neq 0$ and insert it into the matrices M_n . This modification breaks the up-down symmetry of the problem, so that the matrices M_n and L_n have a larger number of distinct matrix elements. This is a straightforward procedure that has been carried out for other models [18, 19]. In the Appendix we present the full set of recurrence maps used in this work.

IV. RESULTS

We study the thermodynamic functions, i.e. the free energy f , the entropy s , the specific heat c , the spontaneous magnetization m and the correlation length ξ as function of the

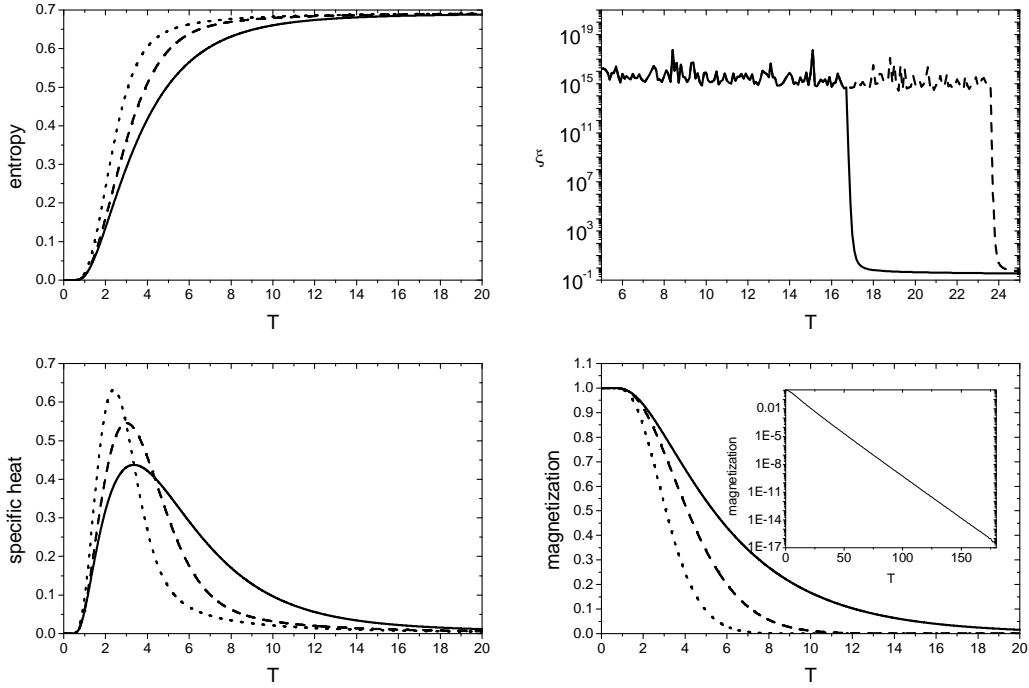


Figure 2

FIG. 2: Thermodynamic functions for the ferromagnetic model. Solid, dashed and dotted lines indicate $\alpha = 0, 1$ and ∞ .

temperature T , as shown in Figures 2 to 5. They were obtained by numerically iterating the set of maps shown in the Appendix, starting with T dependent initial conditions, until a value $n^*(T)$. This temperature dependent value is set automatically, by requiring that one (or a set) of the intensive quantities and/or the correlation length, have converged to a fixed value, within a previously established relative tolerance. This is usually $\sim 10^{-15}$, as we work with double precision variables. Convergence based only on the value of f and its derivatives is much faster than for ξ , specially when the system is in the ordered phase. Otherwise stated, if we call $n_x^*(T), x = f, s, c, m, \xi$, the value of n at which the function x has converged for that particular value of T , then we find that $n_\xi^*(T)$ always assumes the largest value.

In Figure 2 *a, b, c* and *d* we show the entropy s , the specific heat c , spontaneous magnetization $m(h = 0)$ and correlation length ξ , for three distinct values of α , when all coupling constants have ferromagnetic character, i.e., $J_0 > 0$ and $(+1)^n$ in eq.(8). The qualitative

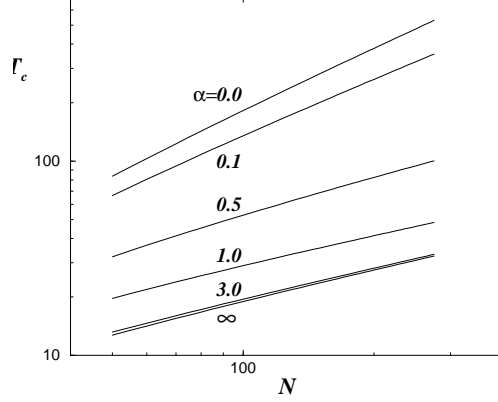


FIG. 3: Size dependent critical temperature for distinct values of α .

behavior does not depend on the values of $\alpha(0, 1, \text{ and } \infty)$, i.e., whether interactions are only short ($\alpha \rightarrow \infty$) or long range ($\alpha = 0$). For all cases we see that, for low values of T , long range correlation sets in, as is evident from the spontaneous magnetization and the numerical divergence of ξ . The remarkable feature, however, points to the absence of any criticality when T is increased. The insert in Fig 2b shows that, when $\alpha = 0$, m goes to zero smoothly, as $\exp(-T)$, with no evidence of a sharp transition to $m = 0$ at a well defined critical temperature. If we consider $\alpha > 0$, we still find a smooth, but stronger, decay, namely as $m \sim \exp(-T^\lambda)$. The curve for the specific heat is also smooth, showing a typical Schottky maximum, again without any evidence of a divergence, that would be expected for a usual phase transition.

The results for the correlation length (d) are also distinct from those found for other scale invariant models, as the diamond hierarchical lattice (DHL)[19]. There, ξ is finite for large values T and numerically diverges for all values of T below a well defined critical value T_c which in our case means attaining a value larger than 10^{16} , the largest allowed number in our algorithm. Within this region, the actual value reached by $\xi(T)$, has no precise meaning. Typically it is much higher than those in the disordered phase, and is also characterized by the presence of random fluctuations. As mentioned before, $n_\xi^*(T)$ is larger than $n_x^*(T)$, $x = f, s, c, m$, but even if we stop the iterations at $n_f^*(T)$, ξ has already reached this very high plateau. This shows that it is not actually necessary to proceed further with the iteration of the maps, as we would obtain only a meaningless value for ξ .

In the present case, if we use $n_f^*(T)$ to stop the iteration of the maps, we observe that ξ

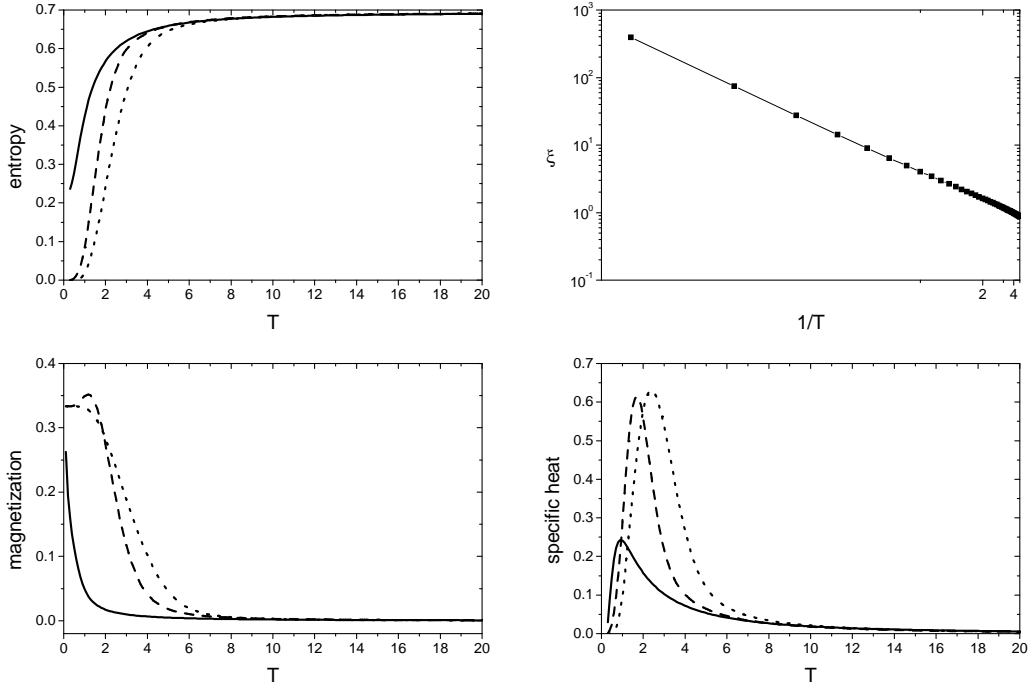


Figure4

FIG. 4: Thermodynamic functions for the anti-ferromagnetic model. Solid, dash and dots indicate $\alpha = 0, 1$ and ∞ . ξ is drawn only for $\alpha = 0$ and reciprocal temperature axis.

diverges at low temperatures, expressing long range order. When T is increased beyond a given value of T^* , it converges to a well defined value, suggesting the break of long range correlation. However, if the iteration procedure is pursued to a value of $n > n_f^*(T)$ we observe that the T interval in which ξ diverges becomes larger. This finding has driven us to proceed with the iteration of the maps in a different way. We fix a value $\bar{n} > n_f^*(T = 1)$, and iterate the maps until reaching \bar{n} for all values within a large T interval, as shown in Figure 2c. Then it is possible to precisely evaluate a critical value $T_c(\bar{n})$, as the value of T where the behavior of ξ changes. In Figure 3 we show how $T_c(\bar{n})$ depends on \bar{n} , for several distinct values of α . Our findings for this unusual kind of critical behavior suggest a power law $T_c(n) \sim n^{\tau(\alpha)}$, with τ going continuously from $\tau(\alpha = 0) = 1$ to $\tau(\alpha = \infty) = 1/2$. We recall that a similar behavior has been reported for spin models on another scale-free lattice [17].

In Figure 4 we show that antiferromagnetic interactions ($J_0 < 0$) change the thermody-

dynamic behavior of the model. The most interesting situation is observed for $\alpha = 0$. All triangles in the lattice are frustrated and, as expected, a residual entropy $s_0 = 0.222$ is measured. This best numerical value is smaller than that for the triangular lattice $s_0 = 0.3238\dots$, [20], and much smaller than that obtained for the Ising model on the Sierpinski gasket $s_0 = 0.493\dots$, (SG)[21, 22, 23].

At the same time we find finite well defined values for ξ for all values of T , which are robust with respect to the value of \bar{n} where the iterations are stopped. This is illustrated in Figure 4d, which also shows that, as $T \rightarrow 0$, ξ decays like $\exp(-1/T)$, typical for the 1-d chain. This is a somewhat unexpected behavior, as the presence of frustration usually does not allow for long range correlation of spin orientation, even at $T = 0$ (e.g. the AF Ising model on the SG [23]). At the same time, this result must be related to the non-vanishing behavior for the magnetization, shown in Figure 4c. It indicates that the number of spins pointing in each direction is not the same. Once again, this behavior is different from that obtained for other frustrated lattices, like the planar triangular lattice or the SG. Finally, the behavior of the specific heat looks like those found when $J_0 > 0$, for any value of α .

In Figure 4 we also draw curves for the thermodynamic functions when $\alpha = 1$, and ∞ . In Figure 4c we see that the magnetization curve always saturates at $m(T \rightarrow 0, h \rightarrow 0) = 1/3$. This indicates that, in this limit, the number of spins pointing in opposite directions is not the same, as is the case for the triangular lattice, but stay in proportion 2/3 to 1/3 independent on α . For some range of values of α , m goes through a maximum (e.g. at $(T, m) = (1.2, 0.351)$) when $\alpha = 1$, so that a reentrant behavior at low temperatures is observed.

Let us also discuss how the presence of interactions with different sign affects the behavior of the system, i.e., when we take $(-1)^n$ in eq.(8). As expected, the result depends whether $J_0 > 0$ or < 0 . In the first case, competition and frustration give rise to residual entropy when $\alpha = 0$, as illustrated in Figure 5a. However we note that the value of s_0 is smaller (~ 0.152) than in the case of equal AF interactions. This happens because not all triangular units are build by an odd number of AF bonds, as we can easily see by inspecting the first generations with the help of Figure 1b. Also for $\alpha = 0$ we note the presence of a double Schottky peak in the specific heat (Figure 5b). For $\alpha \neq 0$ there is no remarkable difference between the curves for s or c with respect to those obtained for interactions with the same sign. The results also show that the low temperature magnetization saturates at the value

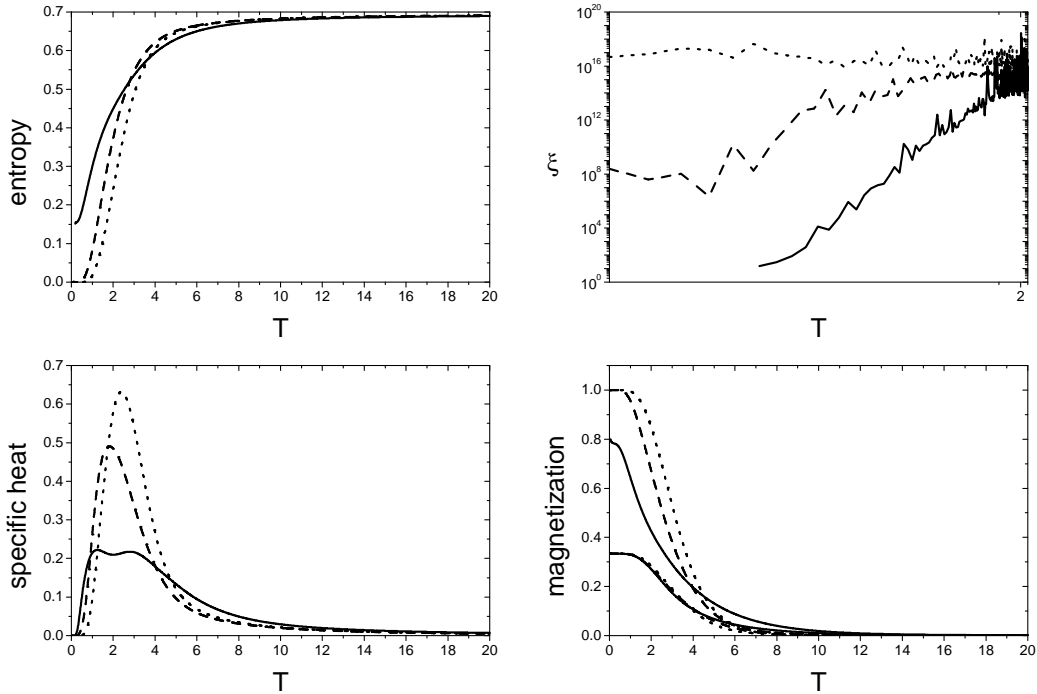


Figure 5

FIG. 5: Thermodynamic functions for the model with alternating ferro and anti-ferromagnetic coupling, starting with $J_0 = 1$. Solid, dash and dots indicate $\alpha = 0, 1$ and ∞ and $J_0 > 0$. In (c) three curves for the magnetization when $J_0 = -1$ and same values of α saturate at $m = 1/3$ are also drawn.

$m = 7/9$ only when $\alpha = 0$, otherwise $m = 1$.

Finally, when $J_0 < 0$ and alternating sign are considered, no frustrated bonds and, consequently, no residual entropy is found. The curves for the specific heat are also smooth like all other cases. The magnetization curves saturate again to $m = 1/3$ as $T \rightarrow 0$ for all values of α . However, reentrant behavior similar to that found for some of the AF cases has not been observed, so that the typical shape is that shown in Figure 5c.

V. CONCLUSIONS

We have studied a family of Ising models on an Apollonian network using the transfer matrix technique. On one hand we considered ferro- and antiferromagnetic couplings and

on the other hand we generalized the interaction as being dependent on the generation as well in the sign as in the strength quantified by an additional parameter α .

For purely ferromagnetic couplings we always find order in the thermodynamic limit independent on α which is in agreement with what has been found on other scale-free lattices[17]. Interestingly the effective critical temperature at which the correlation length diverges goes to infinity with the system size with a power-law in the number of generations with an exponent that depends on α . For antiferromagnetic couplings we find a disordered phase for any finite temperature but a diverging correlation length at $T = 0$. This later observation is unusual as it does not appear for instance on the Sierpinski gasket[23].

Considering the Apollonian network as a model for the connections between cities as described in ref.[14] our result can be applied to the formation of opinions where spin up means one opinion and spin down the other one. The results for the ferromagnetic case implies that independent on the strength of the couplings between the cities as long as it is not zero one single opinion will finally prevail.

If the Apollonian network describes the force lines in a dense polydisperse packing with each particle having a magnetic moment as it is the case in tectonic faults[24] our result for the ferromagnetic Ising model would imply that if all particles have a moment of equal strength one always finds a spontaneous magnetization.

Our calculations can be generalized to random couplings (spin glass) which in fact is work in preparation. One can also imagine studying other more complex magnetic models on the Apollonian networks, like the Potts model, the XY model or the Heisenberg model and one can also study the magnetic properties of Apollonian packings of different topology or higher dimension and even the case of the random Apollonian packing[25].

VI. ACKNOWLEDGEMENT

H.J. Herrmann thanks the Max Planck Research Award Prize. R.F.S. Andrade was partially supported by CNPq.

VII. APPENDIX

The maps for the free energy and correlation length derived from eqs. (12) read:

$$f_{n+1} = \frac{3N_n f_n}{N_{n+1}} - \frac{T}{N_{n+1}} \{3 \ln \alpha_n + \ln \{1 + 3z_n \beta_n (2 + \beta_n) + 3z_n^2 (1 + 2\beta_n (1 + \beta_n)^2) + z_n^3 (1 + 2\beta_n)(2 + \beta_n)^2\} - 6 \ln 2\}, \quad (13)$$

$$\begin{aligned} \xi_{n+1} = \xi_n \{ & 1 + \xi_n \\ & \{ \ln(1 + 3z_n \beta_n (2 + \beta_n) + 3z_n^2 (1 + 2\beta_n (1 + \beta_n)^2) + z_n^3 (1 + 2\beta_n)(2 + \beta_n)^2) - \\ & \ln(z_n^{-1} \beta_n^4 + z_n (1 + 4\beta_n + 2\beta_n^2 + 2\beta_n^3) + z_n^2 (4 + 10\beta_n + 11\beta_n^2 + 2\beta_n^3) + \\ & z_n^2 (3 + 10\beta_n + 10\beta_n^2 + 4\beta_n^3)) \} \}^{-1} \end{aligned} \quad (14)$$

where $z_n = (c_n - d_n)/(c_n + d_n)$, $\alpha_n = p_n + q_n$ and $\beta_n = (p_n - q_n)/(p_n + q_n)$ and $N_n = N(n)$.

-
- [1] Y. Gefen, B.B. Mandelbrot, A. Aharony, Phys. Rev. Lett. **45**, 855 (1980).
 - [2] Y. Gefen, A. Aharony, Y. Shapir, B.B. Mandelbrot, J. Phys. A: Math. Gen. **17**, 435 (1984).
 - [3] A.A. Migdal, Zh. Eksp. Theor. Fiz. **69**, 1457 (1975)
 - [4] A.N. Berker, S. Ostlund, J. Phys. C **12**, 4961 (1979).
 - [5] M. Kaufman and R.B. Griffiths, Phys. Rev. B **24**, R496 (1981).
 - [6] C. Tsallis, A. Magalhães, Phys. Rep. **268**, 305 (1996).
 - [7] C.S.O Yokoi, M.J. de Oliveira, S.R. Salinas, Phys. Rev. Lett. **54**, 163 (1985).
 - [8] J.H. Luscombe, R.C. Desai, Phys. Rev. B **32**, 1614 (1985).
 - [9] B. Bonnier, Y. Leroyer, C. Meyers, Phys. Rev B **37**, 5205 (1988).
 - [10] D.W. Boyd, Can.J.Math. **25**, 303 (1973)
 - [11] H.J. Herrmann, G. Mantica and D. Bessis, Phys. Rev. Lett. **65**, 3223 (1990)
 - [12] R. Mahmoodi Baram, H.J. Herrmann and N. Rivier, Phys. Rev. Lett. **92**, 044301 (2004)
 - [13] J.A. Dodds, J. Colloid. Interface Sci. **77**, 317 (1980)
 - [14] J.S. Andrade Jr., H.J. Herrmann, R.F.S. Andrade, L.R. Silva, cond-mat/0406295 (2004)
 - [15] J.P.K. Doye and C.P. Massen, cond-mat/0407770.
 - [16] G. Oron, H.J. Herrmann, J. Phys. A **33**, 1417-1434 (2000).
 - [17] A. Aleksiejuka, J.A. Holyst and D. Stauffer, Physica A **310**, 260 (2002).
 - [18] M. Kohmoto, L.P. Kadanoff and C. Tang, Phys. Rev. Lett. **50**, 1870 (1983)

- [19] R.F.S. Andrade, Phys. Rev. E **59**, 150 (1999).
- [20] G.H. Wannier, Phys. Rev. B **79**, 357 (1950).
- [21] M.P. Grillon, F.G. B. Moreira, Phys. Lett. A **142**, 22 (1989).
- [22] R.B. Stinchcombe, Phys. Rev. B **41**, 2510 (1990).
- [23] R.F.S. Andrade, Phys. Rev. B **48**, 16095 (1993).
- [24] S. Roux, A. Hansen, H.J. Herrmann and J.-P. Vilotte, Geophys. Res. Lett. **20**, 1499 (1993)
- [25] T. Zhou, G. Yan, P.-L. Zhou, Z.-Q. Fu and B.-H. Wang, cond-mat/0409414